Available online at www.sciencedirect.com
ScienceDirect
Journal of Molecular Graphics and Modelling 26 (2008) 1082–1090
Journal of Molecular Graphics and Modelling
www.elsevier.com/locate/JMGM

Catalytic mechanism of L,L-diaminopimelic acid with diaminopimelate epimerase by molecular docking simulations

L. Brunetti [a], R. Galeazzi [a,*], M. Orena [a], A. Bottoni [b]

[a] *Dipartimento di Scienze e Tecnologie Chimiche, Università Politecnica delle Marche, via Brecce Bianche, I-60131 Ancona, Italy*
[b] *Dipartimento di Chimica "G.Ciamician", Università di Bologna, via Selmi 2, I-40100 Bologna, Italy*

Received 18 June 2007; received in revised form 28 September 2007; accepted 28 September 2007
Available online 5 October 2007

Abstract

Peptidoglycan, a key constituent of bacterial cell walls, is currently the target of broad spectrum antibiotics and a new research field involves both design and synthesis of inhibitors of its biosynthesis. Most bacteria require either lysine, or its biosynthetic precursor, diaminopimelate (*meso*-DAP), as a component of the peptidoglycan layer of the cell wall. In this paper, molecular modelling studies were undertaken in order to shed light on the molecular basis of interaction between (2*S*,6*S*)-diaminopimelic acid (L,L-DAP) (**1**) with its target enzyme DAP-epimerase, since this is a key step in the lysine biosynthetic path leading to (2*R*,6*S*)-diaminopimelic acid (*meso*-DAP) (**2**). In particular, the docking of the ligand–enzyme complex was studied by means of MD simulations and DFT computations in order to ascertain the optimal structural requirements for the epimerization reaction. Molecular dynamics simulations clearly showed that the configuration of the distal carbon C–6 of L,L-DAP is critical for complex formation since both amino and carboxylate groups are involved in H–bonding interactions with the active site residues. Furthermore, the interactions occurring between the functional groups bonded to the C–2 and some residues of the binding cavity immobilize the ligand in a position appropriate for the epimerization reaction, *i.e.*, exactly in the middle of the two catalytic residues Cys73 and Cys217 as confirmed by DFT quantum mechanical computation of the Michaelis complex. All this mechanistic information could be useful for the rational design of new potential antibiotic drugs effective as inhibitors of peptidoglycan biosynthesis.

Keywords: Molecular dynamics; Manual docking; Diaminopimelic acid; Epimerase; DFT

1. Introduction

Bacterial peptidoglycan is a macromolecule which confers strength and rigidity to the cell wall, that are vital for cell viability and osmotic integrity. It is made up of a polysaccharide matrix to which short pentapeptide chains cross-linked to each other are appended [1]. Disruption of this structure is the mode of action of important antibiotics such as penicillins and glycopeptides. Because of the common resistance phenomenon, the search for novel antibiotics and antibiotic targets is of crucial importance renewing the interest in antimicrobial drug development, and particularly the peptidoglycan biosynthetic pathway which provides a potential route to novel antibiotic compounds [2].

In fact, in Gram-positive bacteria the third residue in the peptidoglycan pentapeptide is usually L-lysine, whereas in Gram-negative species it is (2*R*,6*S*)-diaminopimelate [2] (D,L-DAP), which is also an intermediate of the biosynthetic route to L-lysine in bacteria and higher plants, but not in mammals, where the DAP/lysine pathway is missing [2–4]. Thus, inhibitors of this pathway could provide potential antibacterial agents displaying low mammalian toxicity. Diaminopimelate Epimerase (E.C. 5.1.1.7, *dap F*) converts L,L-DAP [(2*S*,6*S*)-DAP] into *meso*-DAP [(2*R*,6*S*)-DAP] in analogy with the pyridoxal-5′-phosphate (PLP)-independent proline, glutamate and aspartate racemases [5–8], which invert the configuration at the α-carbon of an amino acid without the use of a cofactor, metals or reducible keto or imino functionalities. On the other hand, *dap F* differs from these latter racemases, because it can discriminate between two stereocentres since it can interconvert the (2*S*,6*S*)-stereoisomer into the (2*R*,6*S*)-diaminopimelate, being unable however to further epimerise this latter to

* Corresponding author. Tel.: +39 71 2204724; fax: +39 71 2204714.
E-mail address: r.galeazzi@univpm.it (R. Galeazzi).

1093-3263/$ – see front matter © 2007 Elsevier Inc. All rights reserved.
doi:10.1016/j.jmgm.2007.09.005

the (2*R*,6*R*)-DAP [3]. This behaviour is noteworthy, since D,D-DAP is not a substrate for this enzyme, suggesting that the stereochemistry of the non-reacting (distal) C–6 carbon is critical for ligand recognition. Mechanistically similar to the well-studied PLP-independent amino acid racemase [9,10] DAP epimerase uses two cysteine residues. In fact the thiolate form of one of the two cysteines functions as the general base, whereas the other cysteine thiol acts as the general acid (''two-base'' mechanism) [11]. Kinetic and isotopic studies of the reduced active site enzyme suggest that these cysteine residues are Cys73 and Cys217: Cys73 (thiolate) acts as a base deprotonating the α-carbon C–2 while Cys217 (thiol) behaves as an acid reprotonating the resulting planar carbanionic intermediate from the opposite side (Scheme 1) [12].

Furthermore, is worth mentioning that from these kinetic studies [12] carried out at a pH range of 6–9, a pH dependency of the reaction rate was observed and in the proposed mechanism the cysteine residue must be present as the anion form with the negative charge stabilized by the effective positive charge of the N-termini of the α-helix dipole. In fact, the same kinetic studies suggest a reduced pK_a (∼6–7 instead of 8–10) for these cysteinic residues both in the forward and the reverse reaction, which could be ascribed to the previously described stabilization. Therefore at neutral pH these cysteines exist as a rapidly equilibrating thiolate–thiol pair in the presence of the substrate.

In addition, mutagenesis studies support the idea that these two cysteines are the catalytic acid/base residues, being strictly conserved together with surrounding residues among all MurI and other cofactor-independent racemases, including aspartate racemase [13].

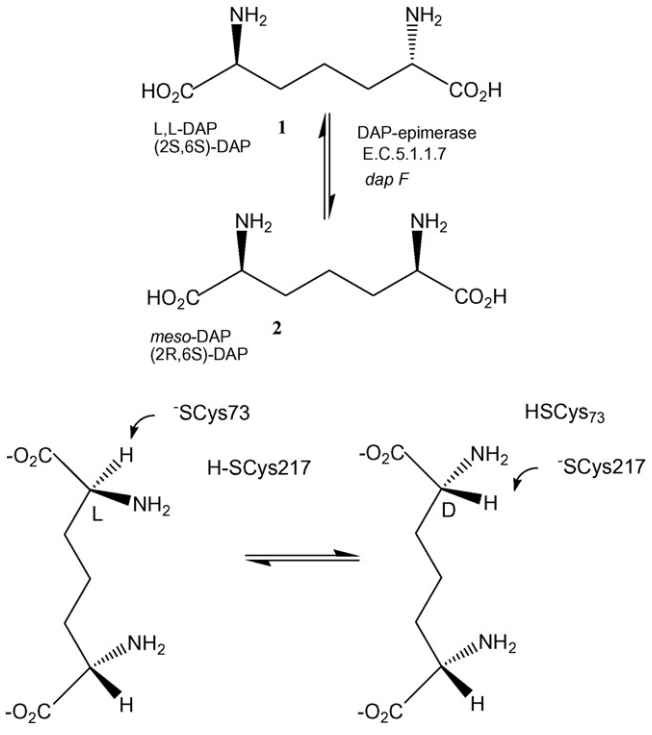

Scheme 1. Epimerization reaction of L,L-diaminopimelic acid (DAP).

Till now neither the mechanism nor the substrate binding modes in the active site have been fully clarified. The crystallographic structure of the enzyme was initially resolved (PDB codes 1 bwz) [14] but it refers to a not well refined 3D structure (2.7 Å) of DAP epimerase from *Haemophilous Influenzae* displaying a disulfide linkage between the two active site cysteines (Cys73 and Cys217) leading to a modified active site that must be built on again, before proceeding to the modelling of the bound substrate. More recently, this X-ray structure was refined (1.75 Å) by Lloyd et al. (PDB code 1 gqz) [15] and the structures of this enzyme in complex with two different isomers of an irreversible active site-directed inhibitor, 2-(4-amino-4-carboxybutyl)-aziridine-2-carboxylate (L,L-and D,L-aziDAP) at high resolution (1.3 and 1.7 Å, respectively) were also obtained (PDB codes 2 gke, 2 gkj) [16].

In these two latter 3D structures both catalytic cysteine residues are present in the active form (Thyolate–Thyol: Cys73-S^- and Cys217-SH in complex with L,L-aziDAP; Cys73 SH and Cys217 S- in complex with L,D-aziDAP) (Scheme 2). However, even if all the knowledge on the binding modes of aziDAP with DAP-epimerase brings a lot of information about the molecular basis of recognition and epimerization, in these crystallographic structures the inhibitor aziDAP is covalently bound with the thiolate basic sulphur atom, which results in the opening of the aziridine ring. On the contrary, the natural ligand forms a classical initial Michaelis–Menten complex before starting the epimerization reaction, suggesting that interaction with the active site residues is strongly different. This is not negligible if the inhibitory ability must be improved by design of a new potential antimicrobic drug. Moreover, at present structural data do not refer to the natural ligand L,L-DAP. Thus, we aimed to elucidate the binding modes of L,L-DAP with DAP-epimerase and to evaluate the strength of the binding complex which could be useful for the rational design of new active compounds.

In addition, detailed structural information on the binding mode of the substrate in the active site is missing, therefore only the anionic form of the cysteinic residue involved as the base (Cys73) in the forward reaction was explicitly considered, since this is a prerequisite for the reaction taking place.

2. Molecular modelling methods

2.1. Conformational analysis procedure

All calculations were carried out on SGI Octane2 IRIX 6.5 workstations. Molecular mechanics calculations were performed using the implementation of AMBER force field (AMBER*) [17] within the framework of Macromodel version 5.5 [18]. The torsional space of each molecule was randomly varied with the usage-directed Monte Carlo conformational search [19]. For each search, at least 1000 starting structures for each variable torsion angle was generated and minimized until the gradient was less than 0.05 kJ/(Å mol). Duplicate conformations and those with an energy in excess of 6 kcal/mol above the global minimum were discarded. The solvent effect was included by using the implicit water GB/SA solvation

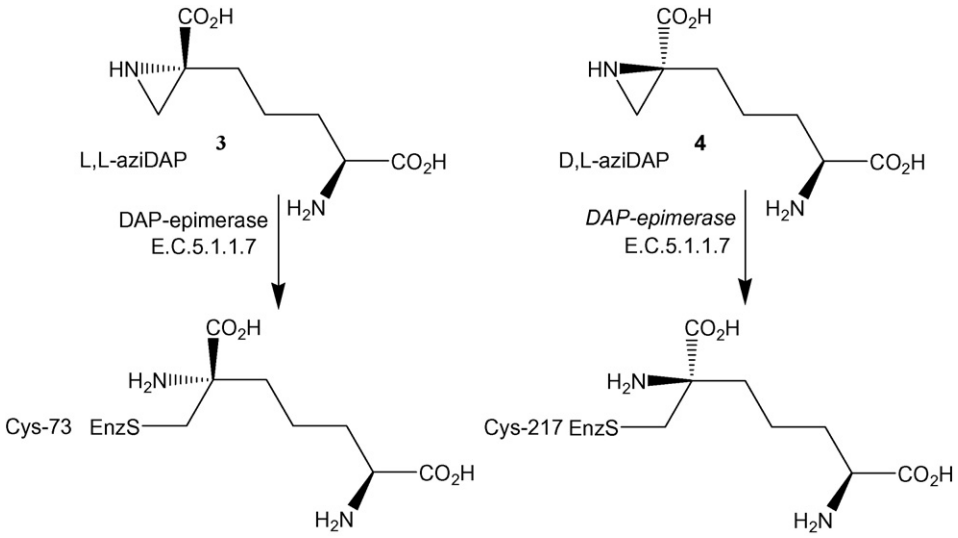

Scheme 2. Inhibition of DAP epimerase by L,L-aziDAP (**3**) and D,L-aziDAP (**4**).

method of Still et al. [20] which takes into account polar solvent effects.

2.2. DFT analysis of the simplified Michaelis complex

All DFT calculations (*i.e.* geometry optimizations and chemical shift simulations) were carried out using the standard tools available in the *Gaussian 98* package, [21] with the DFT/B3LYP functional (*i.e.* Becke's three parameter hybrid functional with the Lee–Yang–Parr correlation functional) [22] with mixed basis set. The B3LYP functional has been demonstrated to provide reliable description of systems including transition metals and involving hydrogen-bond interactions [23,24]. According to this approach the system was partitioned into two regions, which were assigned basis sets of different accuracy. The first region contains the atoms directly involved in the reaction or in the formation of H–bonds and the DZVP basis set was used, whereas the other one includes all the remaining atoms of the active site which were kept frozen during geometry optimization using the small STO-3G basis set [24].

2.3. Docking procedure

The modelling of the L,L-DAP-epimerase complex was performed by means of the MacroModel Ver. 5.5 software package [25]. The energy calculations were carried out with AMBER, as implemented in this package (AMBER*), that uses by default the united atom model [17] providing a special scheme to incorporate specific structural and energetic data directly into the force field. This feature allows to treat explicitly (all-atom model) [26] hydrogen atoms bound to heteroatoms and aromatic carbons. The coordinates of the DAP-epimerase enzyme were retrieved from the Protein Data Bank (PDB code 1 gqz). Then L,L-DAP was properly built and docked into the enzyme active site. Subsequently, the complex underwent a molecular modelling protocol aimed at refining the position of the inhibitor in the active site pocket. Minimization and MD simulations were carried out on a core of unconstrained atoms around the active site (8 Å) and on a shell of constrained atoms (energy penalty force constant of 100 kJ/(Å^2 mol^{-1})) surrounding the core (6 Å). An initial minimization (2000 steps, steepest descent) and a subsequent temperature constant MD simulation (100 ps, 298 K, 1.0 fs time step) were carried out. An equilibration time of 40 ps was allowed before starting the data collection. The MD average structure of the last 60 ps was energy minimized first by steepest descent and then by conjugate gradient with a derivative convergence criterion of 0.05 kJ/(Å^2 mol^{-1}). This molecular modelling protocol already provided reliable results, when studying other inhibitor complexes [27,28].

3. Results and discussion

An understanding of the ligand–protein binding event is critical to subsequently translate structural-based information into more potent and drugable ligands. In this context ''molecular docking'' allows to represent and predict, using computational methods, the mode of interaction of a small molecule when binding to a target protein with a known 3D structure.

The computational investigation on the binding modes of the native substrate was started by using the three-dimensional structure of DAP-epimerase obtained at high resolution (1 gqz). As pointed out previously [16] it is clear that the binding of a ligand into the active site induces a large conformational change in the enzyme. In fact, [16] the most relevant difference in the structure of native and inhibitor bound epimerase is a decreased distance separating the two domains (linked by an S–S bond in the native epimerase) in the latter form. In addition, there is an important coil-to-helix transformation involving residues Gly74-Asn75-Gly76, leading to an additional turn at the N-terminus of helix A (Glu74-Leu86) significatively affecting the active site structure. In fact, a sole catalytic site

results, in which two α-helices (A and B) are related by a pseudo-C2-axis between the two domains, where the two cysteines lie at the N-terminus of each helix.

Before discussing the docking study, the possible protonation pattern of the substrate must be considered. In fact the carboxylate of the ligand must be in the anionic form since protonated α-carboxyl groups of α-amino acids show dramatically reduced pK_a for the Hα (by a factor of about 10^{10}) thus preventing the reaction to occur [29]. This effect can be ascribed to the electrostatic environment of the α-carboxylate which likely disperses its negative charge stabilizing this form and thus amplifying this effect [30]. Hence, the possible state of protonation for L,L-DAP considered in this study are the classical zwitterionic form (prevalent at neutral pH) and the corresponding basic anionic form (prevalent at pH ∼ 8).

Since ligand recognition is a dynamic event where both protein and ligand adopt a definite conformation in order to maximize their interactions, before docking the ligand into the enzyme active site, a full conformational analysis of the ligand alone (L,L-DAP) was carried out, both in the zwitterionic and anionic form, in order to identify all its possible pharmacophoric conformations which represent a good starting geometrical arrangement for the docking process. Thus, all the conformers which lie within 1 kcal/mol from the lowest minimum were considered and tentatively docked into the binding site. Among these, for each protonation state, the only one which could be introduced into the cavity avoiding any destabilizing superimposition of the Van der Waals spheres and which resulted perfectly compatible with the stereoelectronic requirements of the active site (Fig. 1) was choosed.

The structure of the two complexes with L,L-DAP displaying different protonation pattern was subsequently refined by means of a MD run carried out at 298 K for 200 ps using a time step of 0.2 fs leaving the ligand and the active site residues [31] without restraints and keeping the remaining atom coordinates unchanged. The lowest energy structure was eventually energy minimized by using AMBER* FF [17]. Starting from this 3D refined structure, a theoretical model of the Michaelis initial complex was built up by means of quantum mechanical methods using a simplified model of the reaction site, in order to gain more information about the structural requirements of the epimerization reaction. In particular, only the residues of the binding site (Asn11, Phe13, Gln44, Tyr60, Asn64, Val70, Gln72, Cys73, Gly74, Asn75, Asn157, Pro158, His159, Val189, Asn190, Glu208, Arg209, Cys217, Gly218, Ser219, Gly220) were explicitly included, and all the atoms directly involved in the reaction were let free to move while the others were ''frozen'' in their crystallographic position (Fig. 2). The calculations were performed at DFT level of theory by using the B3LYP functional with mixed basis sets (DZVP for all the atoms involved in the reaction and STO-3G for all the others) [32,33].

As a result of this calculation, a minimum structure was obtained in which the αC lies just in the middle of the two cysteine sulphur atoms, being correctly positioned to undergo the epimerization reaction. In fact, the distance (2.57 Å) between the hydrogen H1, which has to be abstracted, and the basic sulphur S1 is very close to that between the αC and the acidic hydrogen H2 (2.72 Å) (Fig. 2). Starting from these data, the docking of the target enzyme (PDB code 1 gzq) in complex with L,L-DAP was performed in order to obtain information on the overall conformation starting from the anionic state of protonation of the latter. Thus, the ligand was manually introduced into the active site in its bioactive conformation according to six possible low energy orientations and the complex was energy minimized using as constraints all the structural data obtained for the DFT optimized Michaelis complex, namely distances $d1 = d$(H2–N), $d2 = d$(S1–αC), $d3 = d$(S_2–αC), $d4 = d$(S1–H1), and angles $a1$ = angle (S2–H2–αC), $a2$ = angle (S1–H1–αC) which were fixed at the values of 2.41 Å, 3.55 Å, 2.71 Å, 2.57 Å, 118.05°, 137.52°, respectively, by using a force constant of 100 kcal/mol Å (Fig. 3). These six ligand–enzyme complexes were studied by means of MD simulations according to the protocol reported in Section 2, keeping the introduced restraints.

The interactions between DAP and residues in the active site at the lowest energy conformation of this complex are reported

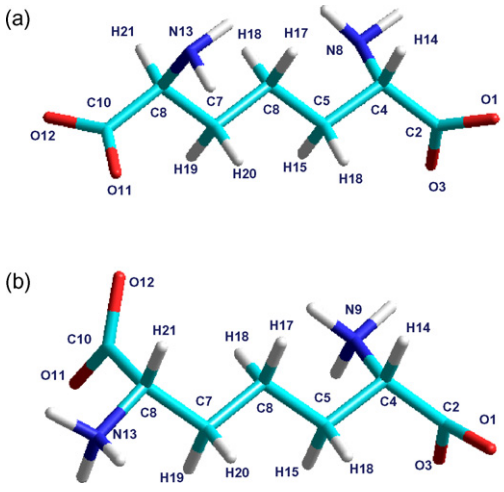

Main torsion angles for L,L-DAP

Torsion angle	anion	zwitterion
O1-C2-C4-N9	-58.29	-42.72
C2-C4- C5-H16	57.35	58.67
H16- C5-C6-H18	-175.15	-176.76
H18- C6- C7- H20	177.27	179.4
H20-C7- C8- H21	175.33	174.45
O11- C10- C8-N13	-57.87	63.96

Fig. 1. Geometry of the bioactive conformation of L,L-DAP (a) in the anionic form (b) in the zwitterionic form.

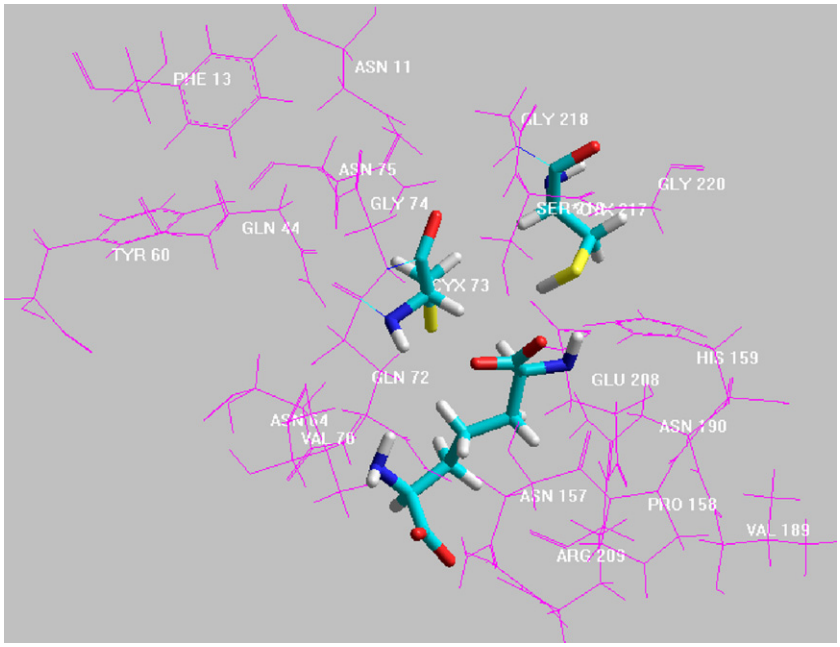

Fig. 2. Residues explicitly considered in DFT calculations. All the residues frozen in their position are shown in pink.

in Fig. 4. Strong H–bonding interactions were observed involving an oxygen of the carboxylate of the epimerizable centre αC of L,L-DAP and three amidic nitrogens of residues Gly74 (d = 1.61 Å), Cys73 (d = 1.63 Å) and Gln72 (d = 1.69 Å), together with a H–interaction between the hydrogen of the amino group at αC and nitrogen of Cys73 (d = 2.55 Å). This latter cannot be considered a true H–bond, but due to its orientation it can be regarded as a polar orientation of the dipoles. Furthermore, the ligand is positioned very close to Val70 and Arg209.

Since the interaction with these latter residues was observed also in our preliminary DFT calculations, the docking was simulated and refined by introducing more distance constraints, namely $d5$–$d6$–$d7$, corresponding to $d5$ = Ser219(O)H–O of COO^- (bonded to α–C) 1.62 Å; $d6$ = Arg209(N)H–O of COO^- (bonded to distal C) 1.69 Å; $d7$ = Arg209(N)H–N(H_2) (bonded to distal C) 2.48 Å. Subsequently, another MD docking simulation was carried out starting from the previous optimized conformation keeping all the geometrical computed restraints. Indeed, a change in the overall energy was observed, which significantly decreased, being associated to a more correct positioning of the ligand inside the cavity and to the consequent presence of an higher number of stabilizing specific interactions. The resulting structure was again minimized removing all

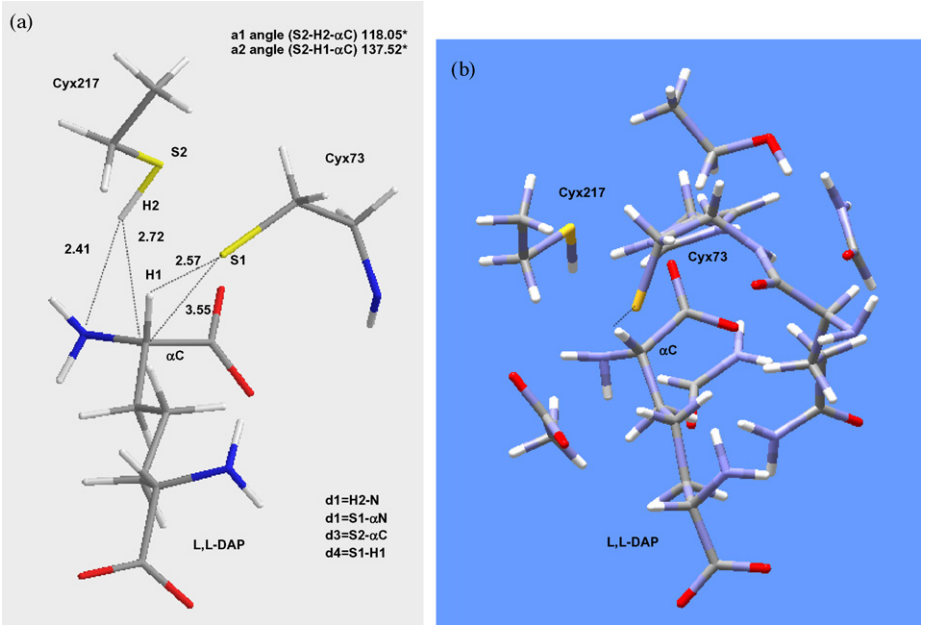

Fig. 3. Structure of the initial Michaelis complex optimized at DFT level of theory.

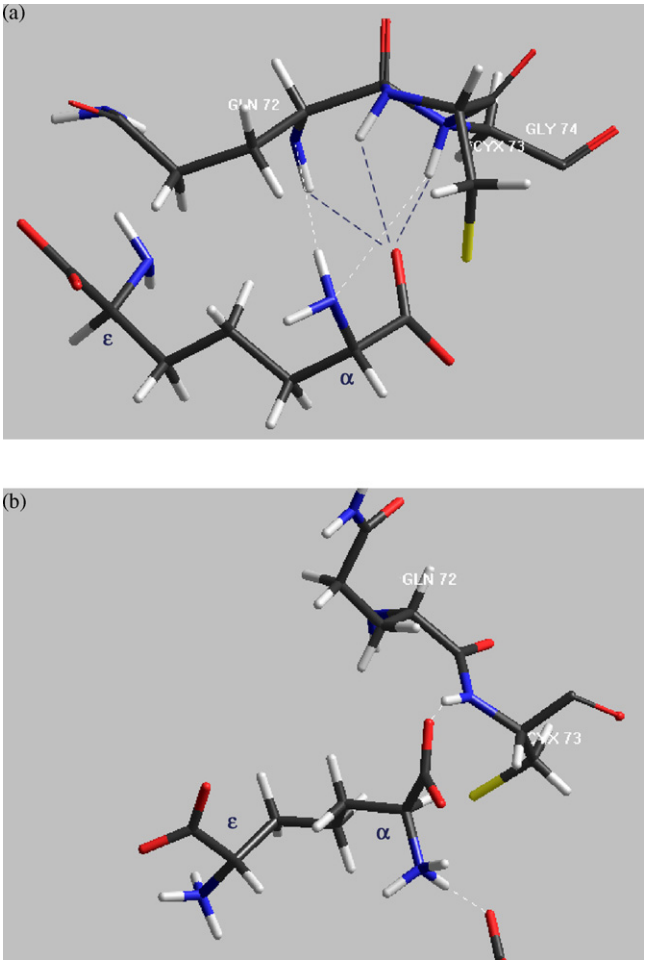

Fig. 4. 3D structure of the lowest energy conformation for L,L-DAP and its target enzyme.

the constraints to let it relax which lead to an overall complex energy of −626.23 kcal/mol (AMBER*) [34]. The same protocol was applied in the docking of the second complex, which involves the enzyme and L,L-diaminopimelate in zwitterionic form. The overall energy obtained in this case for the lowest minimum conformation results −498.18 kcal/mol.

The results of these docking studies were then compared with the structural information already obtained for the inhibitor-epimerase complexes, [16] in order to analyze the main differences in the binding of both the natural ligand and the inhibitor which are very similar in the overall structure, but different in the terminal part of the molecule undergoing epimerization. In fact, when an aziridino ring is included in this part of the molecule, both the conformational arrangements and the stereoelectronic properties (MEP, etc.) significatively change, and different interactions with residues of the active site take place since it covalently interacts with the catalytic residues.

In the inhibitor-epimerase complex, four H–bonds were found directed towards the carboxylate group at the α-carbon undergoing racemization [16]. These are from the main chain nitrogens of residues Gly74, Asn 75, Gly218 and Ser219 and a fifth from O^{γ}-Ser219.

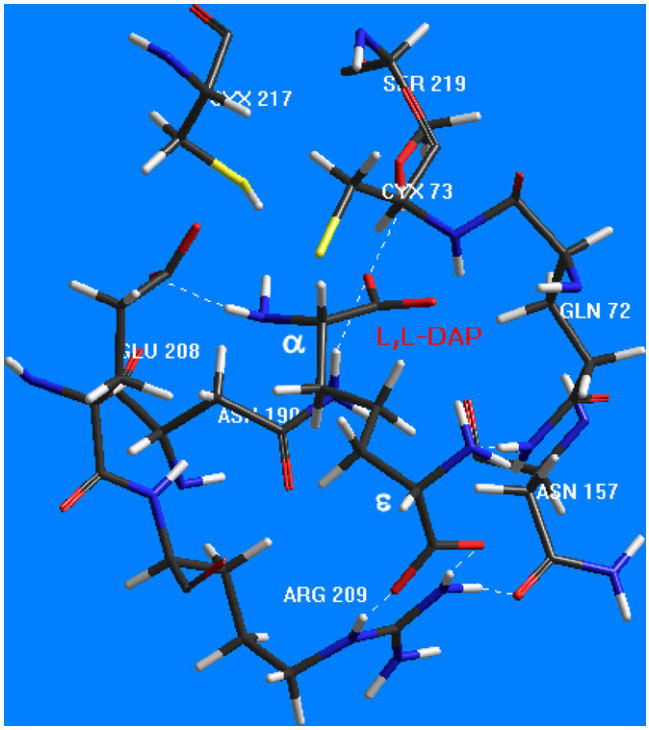

Fig. 5. Molecular H–bonding and non-covalent interactions between L,L-DAP in anionic state of protonation and active site residues in the final docked minimized complex.

The configuration of the distal ε-carbon (L) is critical for substrate recognition since it forms specific interactions with residues of the active site. In the enzyme-L,L-aziDAP complex, these interactions involve a salt bridge with the positively charged side chain of Arg209 along with 3 H–bonds from side

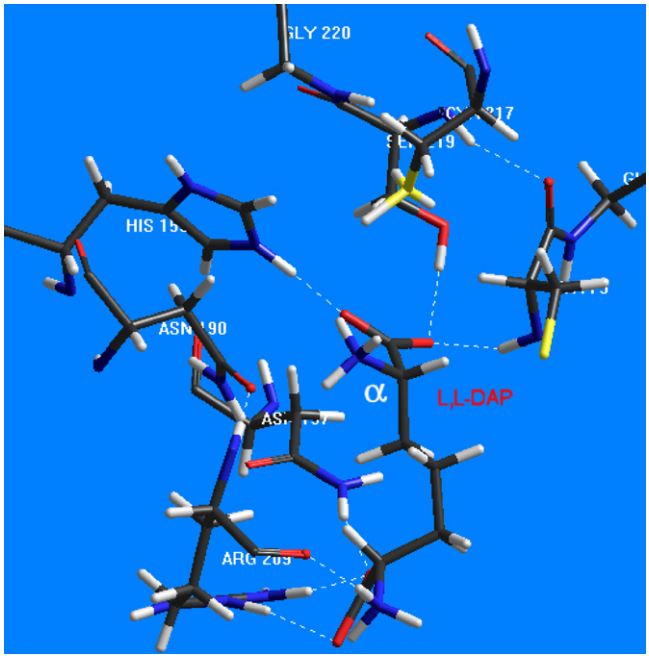

Fig. 6. Molecular H–bonding and non-covalent interactions between L,L-DAP in zwitterionic state of protonation and active site residues in the final docked minimized complex.

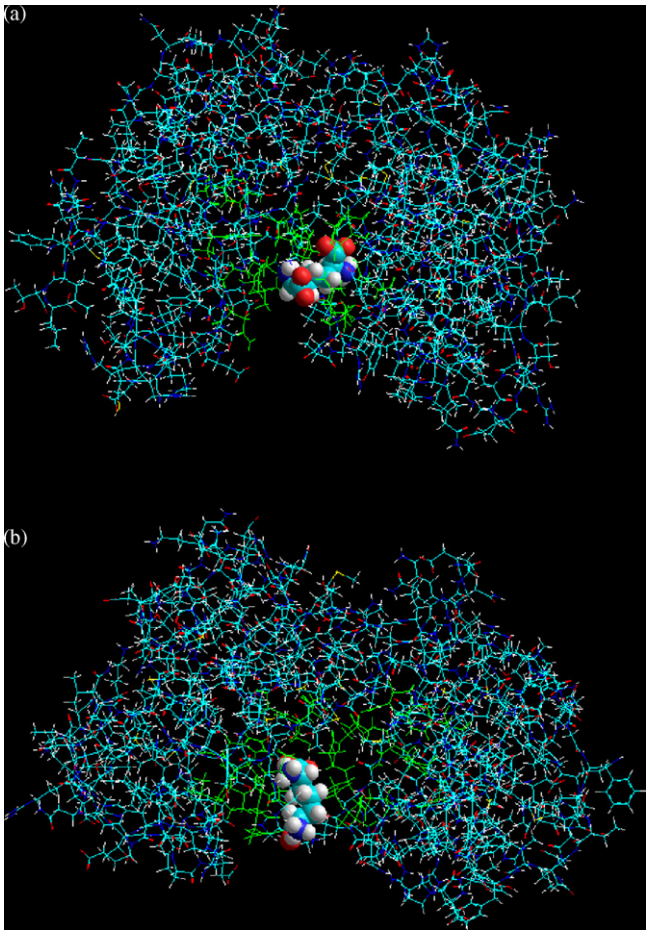

Fig. 7. Final Optimized L,L-DAP–DAP-epimerase complex conformation; diaminopimelate is shown into the cavity in CPK mode; in green are evidenced the active site residues. (a) L,L-DAP in anionic state of protonation (b) L,L-DAP in zwitterionic form.

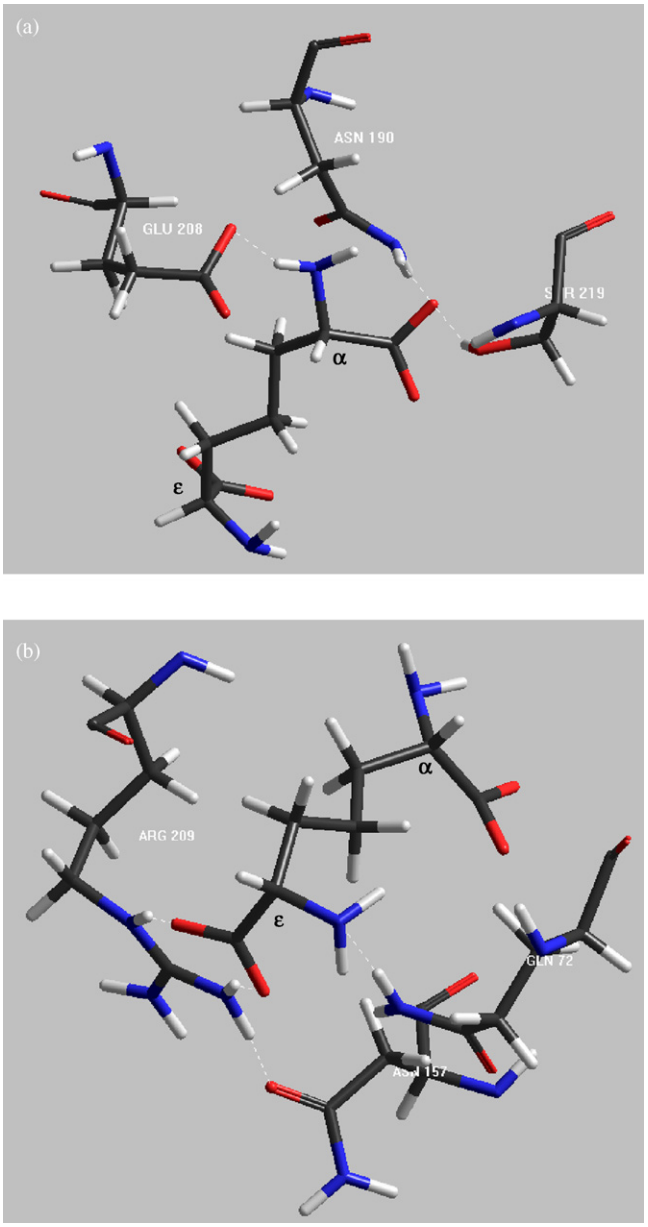

Fig. 8. H–bonding interactions for anionic L,L-DAP involving (a) α-carbon atom (b) distal ε-carbon atom and active site residues.

chains $N^{\delta 2}$ atoms of residues Asn64, Asn157 and Asn190. The amino group is also involved in H–bonding formation with side chain oxygen of Asn64, Glu208 and carboxyl oxygen of Arg209. The asymmetric disposition of Asn64 and Asn157 situated on opposite sides of ε-carbon of the inhibitor, coupled with tight packing of other side residues surrounding the distal site prevents the binding of the D-isomer to that position. The binding interactions of the distal L-stereocentre help in positioning the substrate carbon skeleton correctly for forming the covalent bond between the cysteine sulphur and methylene carbon of L,L-aziDAP.

In the fully minimized structure of the natural complexes the following interactions were observed instead. For the complex with L,L-DAP in the anionic form (Fig. 5, Fig. 7a), the carboxylate of the αC which undergoes epimerization is involved in a symmetric strong double H–bond involving Ser219 OH and Asn190 NH_2 (donors) and the oxygen atom (acceptor) of the DAP αC carboxylate which lies perfectly in the middle of these two residues (Asn190(N)H–O^- 1.73 Å; Ser219(O)H–O^- 1.68 Å) (Fig. 8a). Furthermore, there is a third interaction between the oxygen carboxylate O^-(αC) with Cys73(N)H (d = 2.05 Å). All these specific interactions are strong and ''freeze'' the α-carbon in a definite position close to the catalytic cysteins (in the middle) by blocking its carboxylate group. In fact, it results that the hydrogen atom to be abstracted is positioned just in front of Cys73 S^- (the hydrogen acceptor) (d = 3.26 Å) (Fig. 5). This molecular anchorage is also supported by another specific interaction in which the α-amino group is involved: there is an H–bond between the NH_2 and the carboxylate of Glu208 (d = 1.87 Å). Furthermore, the carboxylate and amino group of the distal carbon are well fixed by strong H–bonding interactions (Fig. 8b) with both oxygens of the carboxylate forming two H–bonds with $^{\gamma}$NH of the Arg209 lateral chain (d = 1.59 Å) and with Gln72 (N)H at 1.65 Å. This latter residue is also blocked in an optimal position to form this H–bonding interaction by Asn157 which contributes to fixing the lateral chain. Finally, the nitrogen N of the amino group

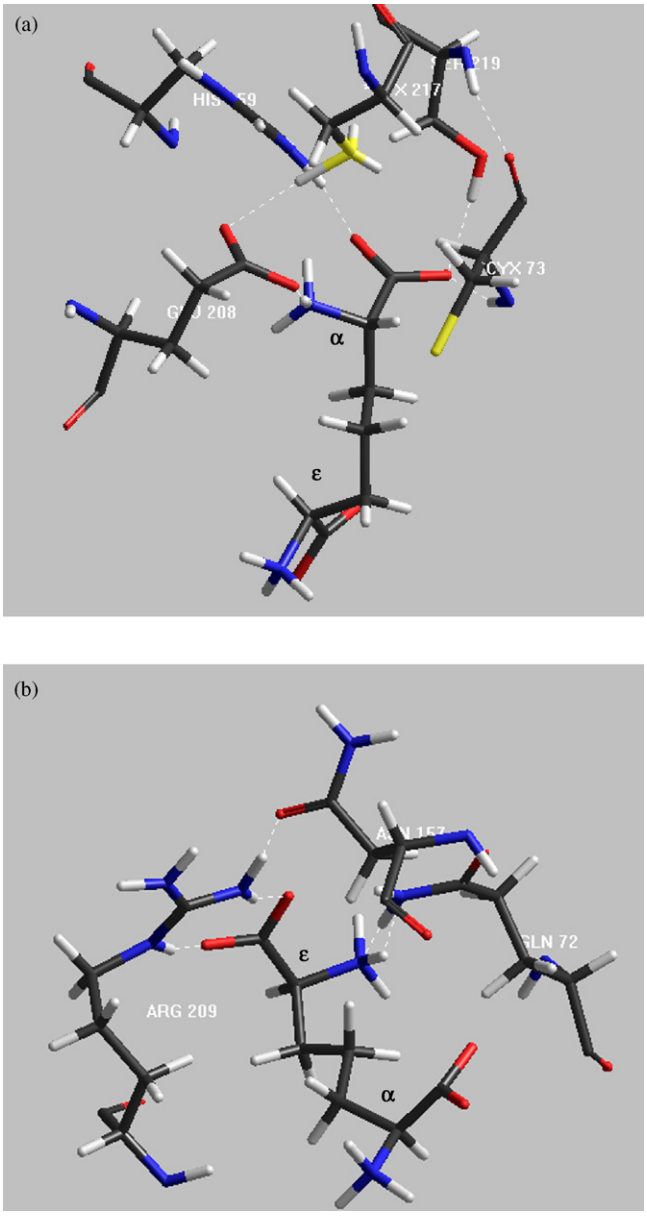

Fig. 9. H–bonding interactions for zwitterionic L,L-DAP involving (a) α-carbon atom (b) distal ε-carbon atom and active site residues.

is also acceptor of another bond which comes from the $^{\gamma}$NH of Gln72.

Analyzing the complex with L,L-DAP in double zwitterionic form (Figs. 6 and 7b), one can observe that in this case too there are many molecular interactions between the ligand and the enzyme involving both terminal ends of diaminopimelate, which result in a strong stabilization. In particular, the carboxylic oxygens (αC) are again involved in three H–bonding interactions: two involving residues Ser219 (OH), Cys73 (NH) as donors and the same oxygen O^- as acceptor (d = 1.84 and 1.86 Å, respectively) and a very strong one between the other oxygen of the carboxylate with His159 (NH) (d = 1.62 Å). Once again, this resulted in "freezing" of the α-carbon in an appropriate position close to the catalytic cysteine as already observed for the complex with anionic L,L-DAP ($d_{\alpha H-S-}$ = 2.95 Å) (Fig. 9a). Furthermore, this orientation is enforced by means of another ionic interaction between NH_3^+ and the carboxylate of Glu208 (d = 1.64 Å), which is itself kept fixed in this position by an internal H–bonding with Cys217 SH. Moreover, the carboxylate and ammonium groups of εC are also frozen by strong H-interactions: the carboxylic oxygens form two H–bonds with the nitrogens of Arg209 lateral chains, as already observed in the anionic complex (d = 1.80 and 1.73 Å) and another one with NH_2 of Asn157 lateral chain (d = 1.77 Å) (Fig. 9b). In the corresponding anionic complex, this latter residue (Asn157) was instead involved in an internal H–bonding with Gln72 which directly interacts with L,L-DAP. Finally, the εC ammonium forms a specific interaction with the Arg209 carboxylate (C=O) of the peptidic backbone.

4. Conclusions

In this molecular modelling study we were able to point out the bioactive conformation of the flexible ligand L,L-DAP which was used to simulate the binding process leading to the epimerization reaction both in anionic and zwitterionic protonation state. Some structural data on the binding was obtained at high-level DFT and used in order to accurately model the docked complex. Subsequently, the specific interactions of L,L-DAP with active site residues were analyzed and particularly strong H–bonding interactions were observed both for the amino (or ammonium) and carboxy group of the α-carbon and of the distal ε-carbon atom, supporting the hypothesis and the experimental evidences that the configuration at this distal atom is critical for activity. From the results collected, it can be concluded that both the ionic states considered (anionic and zwitterionic) form very stable complexes through ionic and H–bonding interactions with almost the same key residues in the catalytic site, even if they are oriented in a slightly different way inside the cavity.

All this molecular information could be a good starting point for the design of a new potent inhibitor and studies of DAP-epimerase in complex with some diaminopimelate analogs are currently underway in our laboratory in order to establish a close relationship between the nature of interactions and the binding affinity.

References

[1] R.J. Cox, A. Sutherland, J.C. Vederas, Bacterial diaminopimelate metabolism as a target for antibiotic design, Bioorg. Med. Chem. 8 (2000) 843–871.
[2] (a) T.D.H. Bugg, Bacterial peptidoglycan biosynthesis and its inhibition, Compr. Natural Prod. Chem. 3 (1999) 241–294;
(b) J.M. Girodeau, C. Agouridas, M. Masson, R. Pineau, F. Le Goffic, The Lysine pathway as a target for a new generation of synthetic antibacterial antibiotics, J. Med. Chem. 29 (1986) 1023–1030.
[3] R.J. Cox, The DAP pathway to lysine as a target for antimicrobial agents, Natural Prod. Rep. 13 (1996) 29–43.
[4] (a) R.M. Williams, G.J. Fegley, R. Gallegas, F. Schaefer, D.L. Preuss, Asymmetric synthesis of (2S,3S,6S)-(2S,3S,6R)- and (2R,3R,6S)-2,3-methano-2,6-diaminopimelic acids, studies directed to the design of novel substrate-based inhibitors of L,L-diaminopimelate epimerase tetrahedron, 52, 1196, pp. 1149–1164.

(b) G. Gottschalk, Bacterial Metabolism, Springer-Verlag, New York, 1979.
[5] M. Antia, D.S. Hoare, E. Work, The stereoisomers of α-diaminopimelic acid. 3. Properties and distribution of diaminopimelic acid racemase, an enzyme causing interconversion of the L,L and meso isomers, Biochem. J. 65 (1957) 448–459.
[6] J.S. Wiseman, J.S. Nichols, Purification and properties of diaminopimelic acid epimerase from *Escherichia coli*, J. Biol. Chem. 259 (1984) 8194–8907.
[7] M.M. Johnston, W.F. Dixen, Studies on amino acid racemases. I. Partial purification and properties of the alanine racemase from *Lactobacillus fermenti*, J. Biol. Chem. 244 (1969) 5414–5420.
[8] N. Nakajima, K. Tanizawa, H. Tanaka, K. Soda, Agric. Chem. Biol. 50 (1986) 2823–2830.
[9] K.A. Gallo, M.E. Tanner, J.R. Knowles, Mechanism of the reaction catalyzed by glutamate racemase, Biochemistry 32 (1993) 3991–3997.
[10] M.E. Tanner, K.A. Gallo, J.R. Knowles, Isotope effects and the identification of catalytic residues in the reaction catalyzed by glutamate racemase, Biochemistry 32 (1993) 3998–4006.
[11] C.W. Koo, A. Sutherland, J.C. Vederas, J.S. Blanchard, Identification of active site cysteine residues that function as general bases: diaminopimelate epimerase, J. Am. Chem. Soc. 122 (2000) 6122–6123.
[12] C.W. Koo, J.S. Blanchard, Chemical mechanism of *Haemophilus influenzae* diaminopimelate epimerase, Biochemistry 38 (1999) 4416–4422.
[13] G. Williams, E.P. Marziarz, T.L. Amyes, T.D. Wood, J.P. Richard, Formation and stability of the enolates of N-protonated proline methyl ester and proline zwitterion in aqueous solution: a nonenzymatic model for the first step in the racemization of proline catalyzed by proline racemase, Biochemistry 42 (2003) 8354–8361.
[14] E. Fritsche, A. Bergner, A. Humm, W. Piepersberg, R. Huber, Crystal structure of L-arginine: inosamine-phosphate amidinotransferase StrB1 from *Streptomyces griseus*: an enzyme involved in streptomycin biosynthesis, Biochemistry 37 (1998) 17664–17672.
[15] A.J. Lloyd, T. Huytn, J. Turkenburg, D.I. Roper, Refinement of *Haemophilus influenzae* diaminopimelic acid epimerase (DapF) at 1.75 Å resolution suggests a mechanism for stereocontrol during catalysis, Acta Crystallogr. D (2004) 397–400.
[16] B. Pillai, M.M. Cherney, C.M. Diaper, A. Sutherland, J.S. Blanchard, J.C. Vederas, M.N.G. James, Structural insights into stereochemical inversion by diaminopimelate epimerase: an antibacterial drug target, Pnas 103 (2006) 8668–8673.
[17] J.S. Weiner, P.A. Kollman, D.A. Case, U.C. Singh, C. Ghio, G. Alagona, S. Profeta, P.A. Weiner Jr., A new force field for molecular mechanical simulation of nucleic acids and proteins, J. Am. Chem. Soc. 106 (1984) 765–784.
[18] F. Mohamadi, N.G.J. Richards, W.C. Guida, R. Liskamp, M. Lipton, C. Caufied, G. Chang, T. Hendrickson, W.C. Still, Macromodel—an integrated software system for modeling organic and bioorganic molecules using molecular mechanics, J. Comput. Chem. 11 (1990) 440–467.
[19] J.M. Goodman, W.C. Still, An unbounded systematic search of conformational space, J. Comput. Chem. 12 (1991) 1110–1117.
[20] W.C. Still, A. Tempczyk, R.C. Hawley, T. Hendrickson, Semianalytical treatment of solvation for molecular mechanics and dynamics, J. Am. Chem. Soc. 12 (1990) 6127–6129.
[21] M.J. Frisch, G.W. Trucks, H.B. Schlegel, G.E. Scuseria, M.A. Robb, J.R. Cheeseman, V.G. Zakrzewski, J.A. Montgomery Jr., R.E. Stratmann, J.C. Burant, S. Dapprich, J.M. Millan, A.D. Daniels, K.N. Kudin, M.C. Strain, O. Farkas, J. Tomasi, V. Barone, M. Cossi, R. Cammi, B. Mennucci, C. Pomelli, C. Adamo, S. Clifford, J. Ochterski, G.A. Patersson, P.Y. Ayala, Q. Cui, K. Morokuma, D.K. Malik, A.D. Rabuck, K. Raghavachari, J.B. Foresman, J. Cioslowski, J.V. Ortiz, A.G. Baboul, B.B. Stefanov, G. Liu, A. Liashenko, P. Piskorz, I. Komaromi, R. Gomperts, R.L. Martin, D.J. Fox, T. Keith, M.A. Al-Laham, C.Y. Peng, A. Nanayakkara, M. Challacombe, P.M.W. Gill, B. Johnson, W. Chen, M.W. Wong, J.L. Andres, C. Gonzales, M. Head-Gordon, E.S. Replogle, J. Pople, Gaussian 98, Revision A. 9, Gaussian Inc., Pittsburgh, PA, 1998.
[22] A.D. Becke, Density-functional thermochemistry. III. The role of exact exchange, J. Chem. Phys. 98 (1993) 5648–5652.
[23] (a) T. Ziegler, Approximate density functional theory as a practical tool in molecular energetics and dynamics, Chem. Rev. 91 (1991) 651–667;
(b) L. Fan, T. Ziegler, Nonlocal density functional theory as a practical tool in calculations on transition states and activation energies. Applications to elementary reaction steps in organic chemistry, J. Am. Chem. Soc. 114 (1992) 10890–10897.
[24] (a) F. Bernardi, A. Bottoni, G.P. Miscione, DFT Study of the palladium-catalyzed cyclopropanation reaction, Organometallics 20 (2001) 2751–2758;
(b) A. Bottoni, A. Perez Higuerelo, G.P. Miscione, A DFT computational study of the bis-silylation reaction of acetylene catalyzed by palladium complexes, J. Am. Chem. Soc. 124 (2002) 5506–5513;
(c) F. Bernardi, M. De Vivo, M. Garavelli, G. Keseru, G. Naray-szabo, A hypothetical mechanism for HIV-1 integrase catalytic action: DFT modelling of a bio-mimetic environment, Chem. Phys. Lett. 362 (2002) 1–7.
[25] N. Godbout, D.R. Salahub, J. Andzelm, E. Wimmer, Optimization of Gaussian-type basis sets for local spin density functional calculations. Part I. Boron through neon, optimization technique and validation, Can. J. Chem.: Rev. Can. Chim. 70 (1992) 560–571.
[26] W.D. Cornell, P. Cieplak, C.I. Bayly, I.R. Gould, K.M. Merz Jr., D.M. Ferguson, D.C. Spellmeyer, T. Fox, J.W. Caldwell, P.A. Kollman, A second generation force field for the simulation of proteins, nucleic acids, and organic molecules, J. Am. Chem. Soc. 117 (1995) 5179–5197.
[27] C. Melchiorre, V. Andrisano, M.L. Bolognesi, R. Budriesi, A. Cavalli, V. Cavrini, M. Rosini, V. Tumiatti, M. Recanatini, Acetylcholinesterase noncovalent inhibitors based on a polyamine backbone for potential use against Alzheimer's disease, J. Med. Chem. 41 (1998) 4186–4189.
[28] A. Rampa, A. Bisi, P. Valenti, M. Recanatini, A. Cavalli, V. Andrisano, V. Cavrini, L. Fin, A. Buriani, P. Giust, Acetylcholinesterase inhibitors: synthesis and structure-activity relationships of ω-[*N*-methyl-*N*-(3-alkylcarbamoyloxyphenyl)-methyl] aminoalkoxy heteroaryl derivatives, J. Med. Chem. 41 (1998) 3976–3986.
[29] J.P. Richard, T.L. Amyes, On the importance of being zwitterionic: enzymatic catalysis of decarboxylation and deprotonation of cationic carbon, Bioorg. Chem. 32 (2004) 354–366.
[30] Z. Zhong, B.J. Postnikova, R.E. Hans, V.M. Lynch, E.V. Anslyn, Large pK_a shifts of α-carbon acids induced by copper(II) complexes, Chem. Eur. J. 11 (2005) 2385–2394.
[31] The residues lying the active site cavity are largely conserved across all the DAP epimerases sequences isolated from different bacterial species and include: Asn11, Phe13, Gln44, Tyr60, Asn64, Val70, Gln72, Cys73, Gly74, Asn75, Asn157, Asn190, Glu208, Arg209, Cys217, Gly218, Ser219, see Ref. [10].
[32] The enzymatic mechanism was also completely studied by localizing all the stationary points involved into the epimerization reaction using the same DFT methods and the results will soon be published.
[33] (a) F. Bernardi, A. Bottoni, M. De Vivo, M. Garavelli, G. Keserü, G. Náray-Szabó, A hypothetical mechanism for HIV-1 integrase catalytic action: DFT modelling of a bio-mimetic environment, Chem. Phys. Lett. 362 (2002) 1–7, This generalized basis set has already provided reliable results as can be seen in;
(b) A. Bottoni, C.Z. Lanza, G.P. Miscione, D. Spinelli, New model for a theoretical Density Functional theory investigation of the mechanism of carbonic anhydrase: how does the internal bicarbonate rearrangement occur? J. Am. Chem. Soc. 126 (2004) 1542–1550.
[34] The enthalpy of binding was calculated by minimizing both the complex then the single isolated enzyme and ligand without any restriction and by using a more well parametrized force field (CHARMM) using the charm22 parametrization. The energy of the complex results −491.20 kcal/mol, the enzyme is −379.50 kcal/mol while l,l-DAP in the binding conformation is 17.33 kcal/mol. The resulting ΔEbinding is 94.37 kcal/mol.